

Evaluation of PVC and PTFE filters for direct-on-filter crystalline silica quantification by FTIR

Bankole Osho, Mohammadreza Elahifard, Xiaoliang Wang, Behrooz Abbasi, Judith C. Chow, John G. Watson, W. Patrick Arnott, Wm. Randolph Reed & David Parks

To cite this article: Bankole Osho, Mohammadreza Elahifard, Xiaoliang Wang, Behrooz Abbasi, Judith C. Chow, John G. Watson, W. Patrick Arnott, Wm. Randolph Reed & David Parks (03 Jul 2024): Evaluation of PVC and PTFE filters for direct-on-filter crystalline silica quantification by FTIR, Journal of Occupational and Environmental Hygiene, DOI: [10.1080/15459624.2024.2357080](https://doi.org/10.1080/15459624.2024.2357080)

To link to this article: <https://doi.org/10.1080/15459624.2024.2357080>



Published online: 03 Jul 2024.



Submit your article to this journal [↗](#)



View related articles [↗](#)




View Crossmark data [↗](#)

REPORT



Evaluation of PVC and PTFE filters for direct-on-filter crystalline silica quantification by FTIR

Bankole Osho^{a,b}, Mohammadreza Elahifard^a, Xiaoliang Wang^a , Behrooz Abbasi^b, Judith C. Chow^a, John G. Watson^a, W. Patrick Arnott^b, Wm. Randolph Reed^c, and David Parks^d

^aDivision of Atmospheric Sciences, Desert Research Institute, Reno, Nevada; ^bUniversity of Nevada, Reno, Nevada; ^cNational Institute for Occupational Safety and Health, Pittsburgh, Pennsylvania; ^dSpokane Mining Research Division, National Institute for Occupational Safety and Health, Spokane, Washington

ABSTRACT

Direct-on-Filter (DoF) analysis of respirable crystalline silica (RCS) by Fourier Transform Infrared (FTIR) spectroscopy is a useful tool for assessing exposure risks. With the RCS exposure limits becoming lower, it is important to characterize and reduce measurement uncertainties. This study systematically evaluated two filter types (i.e., polyvinyl chloride [PVC] and polytetrafluoroethylene [PTFE]) for RCS measurements by DoF FTIR spectroscopy, including the filter-to-filter and day-to-day variability of blank filter FTIR reference spectra, particle deposition patterns, filtration efficiencies, and pressure drops. For PVC filters sampled at a flow rate of 2.5 L/min for 8 h, the RCS limit of detection (LOD) was 7.4 $\mu\text{g}/\text{m}^3$ when a designated laboratory reference filter was used to correct the absorption by the filter media. When the spectrum of the pre-sample filter (blank filter before dust sampling) was used for correction, the LOD could be up to 5.9 $\mu\text{g}/\text{m}^3$. The PVC absorption increased linearly with reference filter mass, providing a means to correct the absorption differences between the pre-sample and reference filters. For PTFE, the LODs were 12 and 1.2 $\mu\text{g}/\text{m}^3$ when a designated laboratory blank or the pre-sample filter spectrum was used for blank correction, respectively, indicating that using the pre-sample blank spectrum will reduce RCS quantification uncertainty. Both filter types exhibited a consistent radially symmetric deposition pattern when particles were collected using 3-piece cassettes, indicating that RCS can be quantified from a single measurement at the filter center. The most penetrating aerodynamic diameters were around 0.1 μm with filtration efficiencies $\geq 98.8\%$ across the measured particle size range with low-pressure drops (0.2–0.3 kPa) at a flow rate of 2.5 L/min. This study concludes that either the PVC or the PTFE filters are suitable for RCS analysis by DoF FTIR, but proper methods are needed to account for the variability of blank absorption among different filters.

KEYWORDS

Coal mine dust; Field Analysis of Silica Tool; Fourier transform infrared; MSHA silica rule; respirable crystalline silica

Introduction

Long-term exposure to respirable crystalline silica (RCS) can cause a range of occupational respiratory diseases including coal workers pneumoconiosis (CWP) and silicosis (Cohen et al. 2022; Vanka et al. 2022). While more stringent regulations and improved dust controls have reduced pneumoconiosis-associated deaths, these diseases continue to be prevalent (Bell and Mazurek 2020; Go et al. 2023). The resurgence of CWP cases in the U.S. central Appalachian regions and a recent outbreak of silicosis among engineering stone workers underscore the importance of continued dust exposure monitoring and reduction (Blackley et al. 2018; Barnes et al. 2019; Hua et al. 2023).

To better protect mine workers from RCS exposure, the Mine Safety and Health Administration (MSHA 2024) published a new rule to reduce the RCS permissible exposure limit (PEL) from 100 $\mu\text{g}/\text{m}^3$ to 50 $\mu\text{g}/\text{m}^3$, which aligns with the non-mining industry PEL promulgated by the Occupational Safety and Health Administration (OSHA 2016). Both regulations specify an action level of 25 $\mu\text{g}/\text{m}^3$, the same as the Threshold Limit Value (TLV[®]) recommended by the American Conference of Governmental Industrial Hygienists (ACGIH[®] 2023). RCS measurement methods must be sensitive enough to reliably quantify at or below the action level.

Coal mine air samples are collected using Coal Mine Dust Personal Sampler Units (CMDPSU) with

polyvinyl chloride (PVC) filters. These filters are sent to designated laboratories for α -quartz (which serves as a proxy for RCS in coal mine dust) analysis by Fourier Transform Infrared (FTIR) spectroscopy following either the MSHA (2008) P7 method or the National Institute for Occupational Safety and Health (NIOSH 2003) 7603 method. These methods involve ashing the particle-laden filter samples to minimize interferences before FTIR analysis and are labor-intensive and time-consuming.

To expedite RCS quantification, NIOSH has been developing a field-based Direct-on-Filter (DoF) RCS measurement method using portable FTIRs (Miller et al. 2012; Hart et al. 2018; Ashley et al. 2020; Pampana et al. 2020; Stach et al. 2020). The DoF technique places the particle-laden filter without pretreatment directly into the infrared (IR) beam. Several data analysis algorithms, including the NIOSH Field Analysis of Silica Tool (FAST) software, are used to quantify RCS on PVC filters (Miller et al. 2017; Chubb and Cauda 2022; Wolfe et al. 2022). This method can provide in-shift or end-of-shift measurements at mining sites with accuracy comparable to laboratory methods (Cauda et al. 2016). The new RCS rules may significantly increase the demand for DoF analyses. However, several factors should be considered for accurate RCS quantification. First, the filter for RCMD sampling and analysis should have low and stable FTIR background interference in the RCS absorption region and such interferences should be corrected. Second, the filter should have high collection efficiencies, low-pressure drops, and high dust-loading capacities (Abbasi et al. 2021; Chow et al. 2022). Third, because only the center portion of the filter is illuminated by the IR beam (diameter 6–9 mm), the particle deposition pattern should be repeatable, and preferably homogeneous, so that a correlation can be established between the FTIR measurement at the filter center and the RCS mass on the entire filter (Miller et al. 2013; Chubb and Cauda 2021, 2022). Fourth, interferences from organics, coal, and other IR-absorbing minerals should be corrected (Miller et al. 2012). This paper addresses the first three factors. Note that FTIR is mainly used for coal mine dust samples, and methods to account for the interference from other minerals in non-coal mines are still under development (Cauda et al. 2018; Wolfe et al. 2022).

Chow et al. (2022) reviewed 12 types of commercially available filter substrates to identify those suitable for mining RCS sampling and FTIR analysis. PVC and PTFE filters exhibit good chemical analysis

compatibility, low gaseous absorption, and minimal interference with RCS spectra. PVC filters are commonly used for dust collection in mining operations, while PTFE filters are often used in ambient air sampling for gravimetric analysis. This study evaluated the impacts of PVC and PTFE filter properties on sampling and DoF FTIR transmittance analysis of RCS, including the variability of blank filter spectra, particle deposition patterns, filtration efficiency, and pressure drop. DoF FTIR uncertainties related to filter variabilities and ways to reduce these uncertainties are discussed.

Materials and methods

Tested filters

PVC and PTFE (also known as Teflon) membrane filters were tested in this study. The 37-mm GLA-5000 PVC filter (SKC Part Number: 225-5-37) has a nominal pore size of 5 μm and a measured thickness of 120 μm (SKC 2024). It has low tare weight and moisture uptake, providing stable gravimetric measurements, and has been widely used for sampling silica, metals, and dust. The 37-mm PTFE filter with a polymethyl-pentene support ring (Cytiva Part Number: R2PJ037) has a nominal pore size of 2 μm and thickness of 46 μm (Cytiva 2024). It is hydrophobic with low moisture uptake, has a low chemical background, and has been widely used for ambient particulate matter sampling. The PTFE filters have higher tare weights than PVC filters.

Laboratory RCS dust generation and collection

RCS particles were collected on filters at different loadings to generate FTIR calibration curves and examine the consistency of particle deposition patterns. The RCS standard uses MIN-U-SIL5 (U.S. Silica), a type of fine ground silica with a nominal mass median diameter of 1.6 μm and silicon dioxide (SiO_2) purity >99.9%. It has been previously used for RCS calibration and testing (Stacey et al. 2009; Miller et al. 2015).

The sampling setup is shown in Figure 1a (Nascimento et al. 2022). Approximately 5 g of MIN-U-SIL5 was placed in a metal bowl which was agitated by a compressed air jet for 5 sec to suspend the dust. Concentrations inside the chamber were monitored by an SPS30 dust sensor (Sensirion) and a DustTrak DRX aerosol monitor (Model 8534; TSI Inc.) (Wang et al. 2009, 2020; Nascimento et al. 2022). Up to four parallel filter packs collected the suspended particles

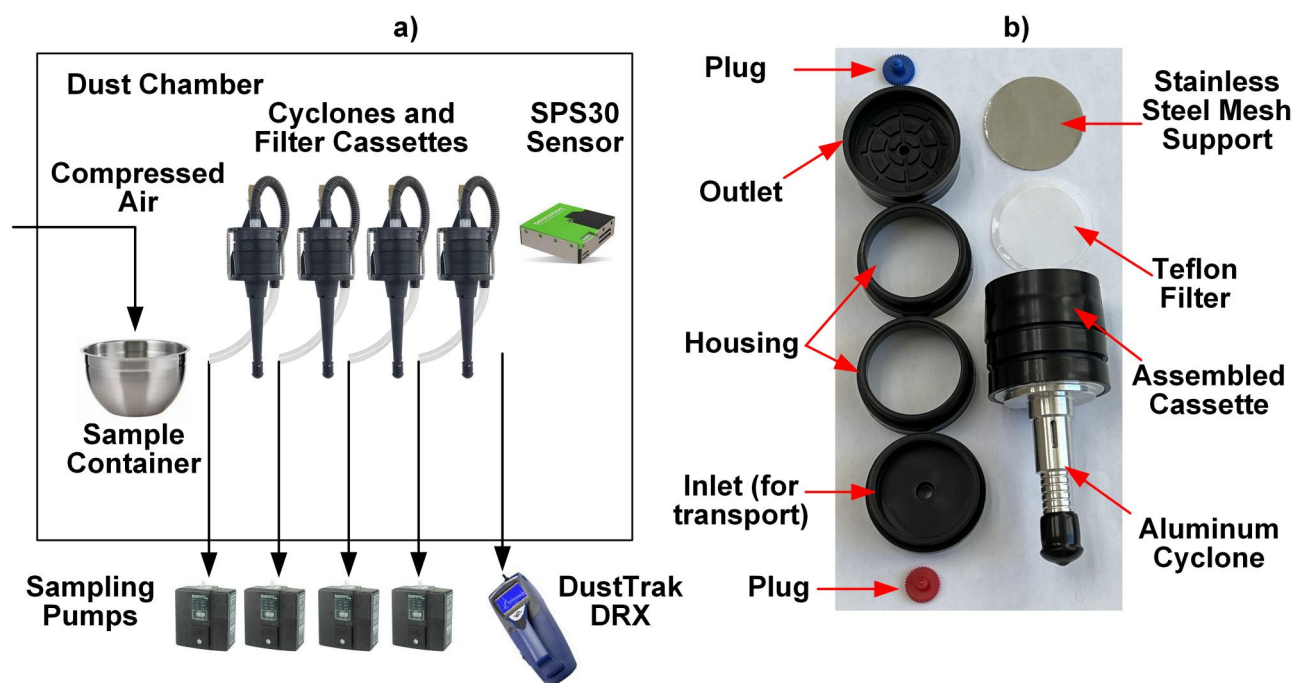


Figure 1. Dust generation and sampling apparatus: (a) sampling train, dust generation, and direct reading instruments; and (b) filter cassette and assembly used for sampling.

for different durations to obtain a range of dust loadings. As shown in Figure 1b, each filter pack consisted of a Zefon respirable dust aluminum cyclone (Part No. ZA0060) with a 50% cut point of $4\ \mu\text{m}$ at 2.5 L/min flow rate and a filter backed by a stainless mesh screen placed in a four-piece conductive polypropylene cassette housing (Part No. 37MMH-4-CF, Zefon) with its outlet connected to a personal sampling pump (Escort ELF, Zefon). The inlet piece of the cassette was only used for transport; therefore, the actual cassette used in sampling had only three pieces. The particle deposition areas with the filter cassette assemblies are $8.9\ \text{cm}^2$ and $7.7\ \text{cm}^2$ for PVC and PTFE filters, respectively, corresponding to a filter face velocity of 4.7 cm/s for PVC and 5.4 cm/s for PTFE at a flow rate of 2.5 L/min. The polymethyl-pentene support ring on the PTFE filter resulted in a smaller deposit area than the PVC filter. The conical expansion of the aluminum cyclone along with the long plenum of the three-piece conductive cassette were expected to reduce particle losses and promote uniform deposits. Filter sampling started once concentrations in the chamber were stabilized as indicated by the SPS30 and DRX. The filters were weighed using an XP6 microbalance (Mettler Toledo Inc.) with a sensitivity of $\pm 1\ \mu\text{g}$ before and after sampling to obtain gravimetric RCS masses, following the quality control and quality assurance (QA/QC) procedure described by Watson et al. (2017). Before weighing, the filters were equilibrated in a temperature ($21.5 \pm 1.5^\circ\text{C}$) and humidity ($35 \pm 5\%$) controlled

environment for at least 24 h to minimize water uptake artifacts.

DoF FTIR analysis and data processing

Most DoF analyses used a VERTEX 70 FTIR spectrometer (Bruker Corp.). A limited number of tests were also conducted with a Nicolet 380 FTIR (Thermo Scientific) to compare data obtained from different FTIR units. Filters were installed in 3D-printed holders which allowed for reproducible positioning in the FTIR chamber. Before each measurement, the FTIR chamber was purged with clean nitrogen for three minutes to remove water vapor and carbon dioxide interferences. An automatic alignment was performed to ensure the instrument's performance. Measurements used the absorbance mode with a spectral resolution of $4\ \text{cm}^{-1}$ over a range of $4000\text{--}400\ \text{cm}^{-1}$. Readings were averaged over 16 scans for each filter, and the Blackman-Harris apodization was used. The absorption (A) by the deposit on each filter sample was calculated as:

$$A = -\ln(T_{\text{Sample}}/T_{\text{Reference}}) \\ = -\ln\left(\frac{I_{\text{Sample}}}{I_{0,\text{Sample}}} \bigg/ \frac{I_{\text{Reference}}}{I_{0,\text{Reference}}}\right) \quad (1)$$

where T_{Sample} and $T_{\text{Reference}}$ are the light transmittance, and I_{Sample} and $I_{\text{Reference}}$ are the transmitted light intensity through the sample filter and a reference

blank filter, respectively. The reference filter can be either the same filter before sampling (referred to as the pre-sample filter) or a designated laboratory blank. $I_{0,Sample}$ and $I_{0,Reference}$ are the incident light intensities (measured with an empty transmittance compartment without a particulate filter) during sample and reference filter measurement, respectively. When the sample and reference filters are measured sequentially, the incident IR intensity can be assumed to be the same, i.e., $I_{0,Sample} = I_{0,Reference}$. Equation (1) can then be simplified as:

$$A = -\ln(I_{Sample}/I_{Reference}) \quad (2)$$

PVC and PTFE filter media have low but non-negligible absorption in the RCS doublet region (Lorberau 1990; Farcas et al. 2016). Therefore, a reference filter spectrum is needed to correct the IR absorption by the pre-sample filter (Chubb and Cauda 2022). The differences in absorption between the pre-sample and reference filters would lead to RCS measurement uncertainties, which were evaluated through blank filter-to-filter and day-to-day spectral variations.

RCS quantification was conducted using the NIOSH FAST method (Chubb and Cauda 2022), which applies six steps: (1) collect the reference spectrum from the pre-sample filter or a designated laboratory blank filter; (2) collect the sample spectrum and correct for the reference filter influence (done by the FTIR software); (3) execute a baseline correction using the concave rubber band method as suggested by FAST; (4) perform integrations of the absorption area for the quartz doublet ($816\text{--}767\text{ cm}^{-1}$; Q-value) and kaolinite band ($930\text{--}900\text{ cm}^{-1}$; K-value); (5) conduct interference corrections for kaolinite if present; and (6) calculate the RCS mass from the kaolinite-corrected quartz doublet area and the sampler-specific calibration equation. The calibration equations were derived by linear regression of RCS absorption area (Q-value) against gravimetric mass.

Filtration efficiency and pressure drop measurement

Filtration efficiencies and pressure drops were measured using the experimental setup in Figure 2 (Soo et al. 2016). Sodium chloride (NaCl) particles were generated by nebulizing a 0.5% aqueous salt solution using a constant output atomizer (Model 3076, TSI Inc.). After drying with a diffusion dryer and charge neutralization using a Kr-85 source (Model 3077A, TSI Inc.), particles were delivered to the test or bypass route. The flow rate through the test section was controlled to 2.5 L/min.

Downstream of the test section, a vacuum removed 2 L/min flow so that only 0.5 L/min was sent through the differential mobility analyzer (DMA; TSI Model 3071). The DMA aerosol and sheath flow rates were set to 0.5 and 5 L/min, respectively, and the DMA voltage scanned from 10 V to 10 kV to select particles in the mobility diameter range of $0.012\text{--}0.32\text{ }\mu\text{m}$, which is equivalent to aerodynamic diameter of $0.018\text{--}0.47\text{ }\mu\text{m}$ (NaCl density 2.16 g/cm^3), over a scan time of 120 s. A condensation particle counter (CPC; TSI Model 3010) measured the particle concentrations downstream of the DMA. The CPC flow (1 L/min) consisted of 0.5 L/min from the DMA and 0.5 L/min from the dilution flow. The DMA and CPC formed a scanning mobility particle sizer (SMPS) (Wang and Flagan 1990) that measured mobility size distributions of particles from the bypass flow or downstream of the filter. The CPC concentrations were corrected for coincidence errors (Jaenicke 1972). Tests were repeated for three filters of each type and each filter was measured three to four times. The pressure drop across the test filter was measured with a digital manometer (Leaton, accuracy: $\pm 0.3\%$ of full scale).

The filtration efficiency (η) for particle diameter i was calculated as:

$$\eta_i = \left(1 - \frac{C_{i,test}}{C_{i,bypass}}\right) \times 100\% \quad (3)$$

where $C_{i,test}$ and $C_{i,bypass}$ are the number concentrations of a particle with diameter i when the flow passes through the test or bypass section.

Results and discussion

Calibration curves for DoF FTIR analysis

The peak integrals (Q-values) were regressed against the different RCS mass loadings to create calibration curves. Due to variations in background absorption with filter media and differences in deposition patterns with both filter and sampler types, the calibration factor is unique for each combination of filter and sampler. The FAST software contains a library of samplers (including different cyclones, cassettes, and filters) and calibration factors (Chubb and Cauda 2022). However, it currently does not include calibration factors for PVC and PTFE filters without the stainless-steel support. Therefore, calibration curves for the sampling setup in Figure 1b were developed.

As shown in Figure 3, the slopes (S) of calibration curves forced through the origin for PVC and PTFE filters are $0.0034\text{ }\mu\text{g}^{-1}$ and $0.0042\text{ }\mu\text{g}^{-1}$, respectively. The higher slope of the PTFE filter is partially caused by the about 13% lower deposition

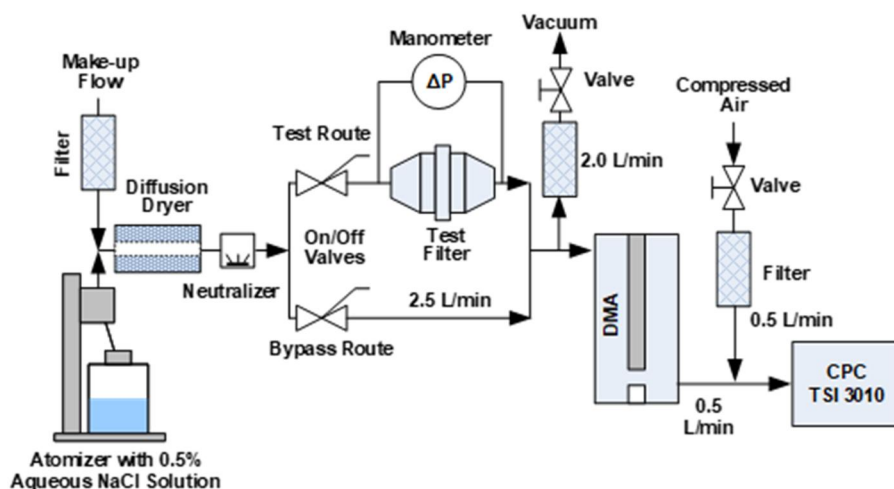


Figure 2. Experimental setup for filtration efficiency and pressure drop tests.

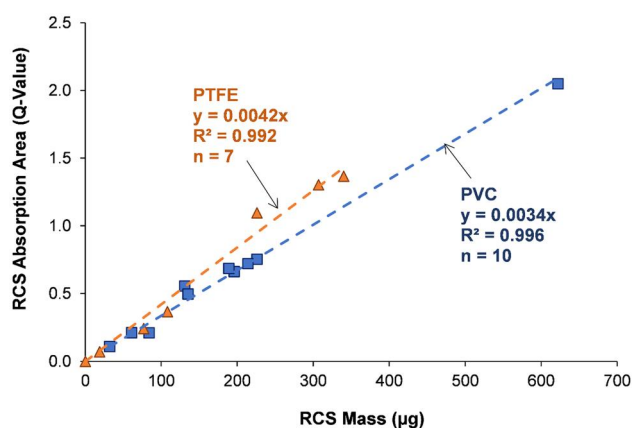


Figure 3. Calibration curves for PVC and PTFE filters with the integrated absorption peak areas (Q-values) linearly regressed with RCS mass loadings.

area, resulting in a higher particle loading per unit of area. As the RCS mass is calculated by the ratio of Q/S, the small S values indicate that small errors in the Q-value may lead to large uncertainties in RCS mass. The S values in the FAST database range from 0.0043 to 0.0077, with $S = 0.0049$ for the Zefon aluminum cyclone and 3-piece cassette sampler (Chubb and Cauda 2021), higher than those in Figure 3. The FAST calibration used 37-mm PVC filters with a stainless-steel ring backing support, which will likely result in a lower deposition area and a higher deposition density than the mesh backing (Figure 1b) used in this study.

RCS uncertainties due to blank filter-to-filter and day-to-day variations of reference spectra

PVC filters

Fifty blank 37-mm PVC filters from the same batch were weighed, showing a mass range of 12.535–

15.037 mg. These filters were allotted to 10 groups of 5 filters in a decreasing mass order. One filter was randomly picked from each group for FTIR measurement, along with another filter with a 14.347 mg mass from the same batch as the reference. The absorption spectra for these 10 blank filters and the reference filter were measured on the same day, and this experiment was repeated on five separate days. Figure 4a shows the absorption spectra (obtained using Equation (2)) over $1,000\text{--}700\text{ cm}^{-1}$ for the 10 blank filters. These filters had similar spectral patterns but with different absorbance amplitudes. When focused over the quartz doublet spectral range of $816\text{--}767\text{ cm}^{-1}$, Figure 4b shows that the absorbance increased with increasing blank PVC filter mass, which was attributed to the increasing filter thickness, by the Beer-Lambert law.

Table 1 shows the Q-values for the 10 blank filters measured on five different days. The negative values indicate that the blank spectra were below the baseline (Chubb and Cauda 2022), which would reduce the calculated RCS absorption area when the sample contains RCS. The filter-to-filter variations of the Q-value, as represented by the standard deviations shown on the bottom row of Table 1, were 0.01 for all 5 days, resulting in an overall standard deviation of 0.01. With the PVC filter calibration factor of $0.0034\text{ }\mu\text{g}^{-1}$ in Figure 3, the equivalent standard deviation of RCS mass was $2.9\text{ }\mu\text{g}$. The day-to-day variations of the Q-value, as represented by the standard deviations shown in the rightmost column of Table 1, were 0.001–0.002 for most samples but with a maximum of 0.008, equivalent to $2.4\text{ }\mu\text{g}$. Estimating the limit of detection (LOD) as three times the blank level standard deviation (U.S. EPA 2016), the LODs for RCS analysis using DoF FTIR with 37-mm PVC filters

are $8.8 \mu\text{g}$ (different filters for reference and sampling) and $7.1 \mu\text{g}$ (same filter for reference and sampling) due to filter-to-filter and day-to-day variation, respectively. These LODs are higher than the $5 \mu\text{g}$ reported

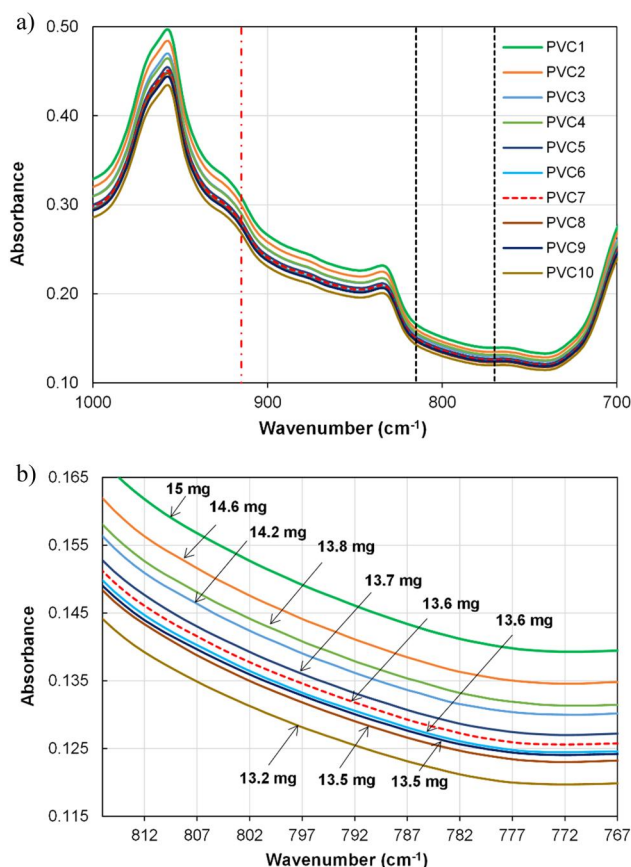


Figure 4. FTIR transmission spectra for 10 blank PVC filters from the same batch measured on the same day, plotted over a spectral range of (a) $1000\text{--}700 \text{ cm}^{-1}$ and (b) $816\text{--}767 \text{ cm}^{-1}$. The vertical black dash lines in panel (a) indicate the crystalline silica absorption doublet region between 816 and 767 cm^{-1} , and the red dash-dot line shows the kaolinite absorption peak at 915 cm^{-1} for interference correction. Associated blank filter mass is noted on panel (b).

by Cauda et al. (2016) and $6\text{--}7 \mu\text{g}$ by Ashley et al. (2020) using the DoF FTIR method. The nominal LODs for the compliance methods involving filter ashing are $5 \mu\text{g}$ for NIOSH 7603 and $1.2 \mu\text{g}$ for the MSHA P7 method (NIOSH 2003; MSHA 2008), similar to those reported by Farcas et al. (2016) ($0.52\text{--}1.5 \mu\text{g}$) and several commercial laboratories ($1.5 \mu\text{g}$) (MSHA 2024). With a flow rate of 2.5 L/min and 8-h sampling, the equivalent LODs for RCS would be $7.4 \mu\text{g/m}^3$ (different filters for reference and sampling) and $5.9 \mu\text{g/m}^3$ (same filters for reference and sampling). The limits of quantification (LOQs; taken as 3.3 times the LODs) are 24.5 and $19.6 \mu\text{g/m}^3$, which are marginally adequate for the action level of $25 \mu\text{g/m}^3$. Table 1 indicates that the mass difference between the pre-sample and reference filters could be an important source of filter-to-filter variation in absorbance. Therefore, selecting a reference filter with a mass close to that of the pre-sample filter would reduce uncertainties. This is demonstrated by the near zero Q-values for the PVC filter with 14.218 mg mass (third filter in Table 1), which had a similar mass to the reference filter (14.347 mg).

The effects of blank filter absorption variations, when used as reference filters, on RCS quantification were further evaluated using a 37-mm PVC filter loaded with $84 \mu\text{g}$ RCS. Nine blank filters with different masses were used as $I_{\text{Reference}}$ in Equation (2) and the measurements were repeated over 3 days. As shown by the circular and triangular symbols in Figure 5, the Q-value increased with the reference filter mass. This result is consistent with the data in Table 1 because the reference blank filter Q-value decreased with filter mass and the Q-value for RCS (calculated as the difference between the sample and reference filter Q-values) increased with reference filter mass. The same tests were repeated on a Nicolet 380 FTIR to evaluate the influence of different FTIR

Table 1. Integrated RCS absorption peak areas over $816\text{--}767 \text{ cm}^{-1}$ (Q-values; unitless) calculated by the NIOSH FAST method for 10 blank PVC filters measured over 5 days.

PVC Filter Mass (mg)	Day 1	Day 2	Day 3	Day 4	Day 5	STDEV (Day-to-Day)
15.037	−0.013	−0.012	−0.014	−0.011	−0.013	0.001
14.576	−0.008	−0.008	−0.004	−0.007	−0.006	0.002
14.218	0	−0.001	0.001	0	0.001	0.001
13.845	0.009	0.007	0.006	0.008	0.009	0.001
13.740	0.011	0.01	0.012	0.011	0.01	0.001
13.647	0	0.011	0.013	0.012	0.011	0.005
13.636	0.014	0.012	0.011	0.014	0.013	0.001
13.530	0.01	0.011	0.013	0.011	0.012	0.001
13.487	−0.002	0.018	0.016	0.015	0.016	0.008
13.181	0.019	0.019	0.018	0.017	0.018	0.001
STDEV (Filter-to-Filter)	0.010	0.010	0.010	0.010	0.010	Overall: 0.010

The reference filter had a mass of 14.347 mg . The filter-to-filter and day-to-day standard deviations (STDEV) are also listed. The negative values are caused by the spectral area being under the baseline.

instruments. Figure 5 shows that the Nicolet FTIR had a similar trend but with a different linear regression equation. The regression slopes of 0.0154–0.0172 indicate that a 1 mg reference filter mass increase would translate to an increase of 4.5–5.1 μg RCS loading or 3.8–4.2 $\mu\text{g}/\text{m}^3$ for an 8-h sampling at 2.5 L/min.

PTFE filters

Twelve PTFE filters from the same batch with masses ranging from 89.896–105.183 mg were selected for Q-value comparison over 5 days. Table 2 shows that the filter-to-filter Q-value standard deviations were about 0.02, which corresponded to 4.8 μg RCS based on the calibration slope in Figure 3. The LOD is 14.3 μg or 12 $\mu\text{g}/\text{m}^3$ and the LOQ is 47.6 μg or 40 $\mu\text{g}/\text{m}^3$ for an 8-h shift sample. These values are 62% higher than those for PVC filters. Unlike PVC blank filters, there is no correlation between the Q-value and blank PTFE filter mass.

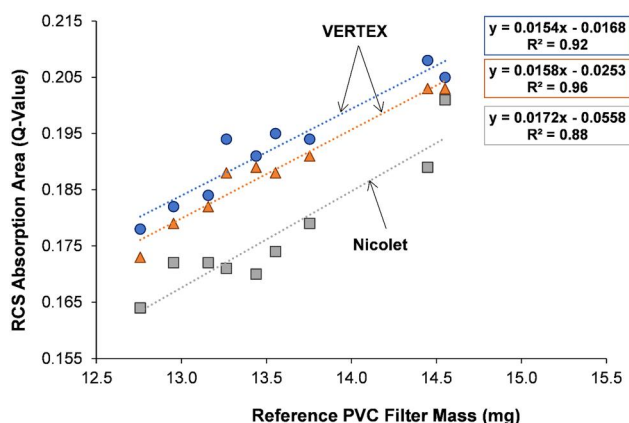


Figure 5. RCS absorption peak integrals in the 816–767 cm^{-1} range (Q-value) obtained by the NIOSH FAST method for a PVC filter loaded with 84 μg RCS using nine different reference PVC filters for blank correction. The results were obtained over three different calendar days by a Bruker Vertex 70 FTIR (circle and triangle symbols) and by a Thermo Scientific Nicolet 380 FTIR (square symbols).

PVC and PTFE filters are structurally different: the PVC filters have a blank mass of about 14 mg without a support ring, while the PTFE filters have a blank mass of about 100 mg with a support ring. The mass of the support ring is much greater than the PTFE membrane itself; therefore, the PTFE filter-to-filter mass variations are likely dominated by the ring rather than the membrane, masking the Q-value changes with membrane thickness. On the other hand, Table 2 shows that the day-to-day standard deviations were ≤ 0.002 , 10 times lower than the filter-to-filter variations. This indicates that using the blank PTFE filter before sampling as an FTIR reference would result in an LOD of 1.2 $\mu\text{g}/\text{m}^3$ and an LOQ of 4.0 $\mu\text{g}/\text{m}^3$.

Table 3 shows the effects of reference PTFE filter variation on the quantification of RCS. Three blank filters with masses ranging from 89.896–105.183 mg (which bracket the filter mass range in Table 2) were used as references for a PTFE filter loaded with 96 μg RCS over 3 days. Unlike the good correlations between RCS Q-values and blank PVC filter mass in Figure 5, no correlations were found for PTFE filters, likely due to the variations of the support ring mass. Similar to the PTFE blank filter data in Table 2, the filter-to-filter Q-values have a standard deviation of about 0.02, while the day-to-day variations were 4–7

Table 3. Integrated RCS absorption peak area over 816–767 cm^{-1} (Q-values; unitless) obtained by the NIOSH FAST method for a PTFE filter loaded with 96 μg RCS using three different blank PTFE filters as reference.

Reference filter mass (mg)	Day 1	Day 2	Day 3	STDEV (Day-to-Day)
89.896	0.408	0.402	0.403	0.003
99.194	0.383	0.38	0.377	0.003
105.183	0.423	0.423	0.415	0.005
STDEV (Filter-to-Filter)	0.020	0.022	0.019	Overall: 0.018

The loaded and reference filters are from the same batch. Measurements were repeated over 3 days.

Table 2. Integrated RCS absorption peak areas over 816–767 cm^{-1} (Q-values; unitless) obtained by the NIOSH FAST method for 12 blank PTFE filters measured over 5 days.

PTFE Filter Mass (mg)	Day 1	Day 2	Day 3	Day 4	Day 5	STDEV (Day-to-Day)
89.896	0.032	0.03	0.031	0.03	0.03	0.001
92.823	0.017	0.018	0.02	0.017	0.017	0.001
95.000	−0.004	−0.002	−0.002	−0.004	−0.003	0.001
95.633	0.004	0.004	0.002	0.003	0.005	0.001
96.855	−0.012	−0.009	−0.008	−0.011	−0.01	0.002
98.880	0.029	0.031	0.033	0.031	0.031	0.001
99.194	0.059	0.053	0.057	0.059	0.058	0.002
100.014	0.046	0.046	0.045	0.048	0.047	0.001
102.534	0.017	0.015	0.018	0.018	0.017	0.001
103.416	0.033	0.032	0.034	0.034	0.035	0.001
103.472	0.026	0.026	0.025	0.024	0.026	0.001
105.183	0.016	0.014	0.015	0.014	0.014	0.001
STDEV (Filter-to-Filter)	0.020	0.019	0.019	0.020	0.019	Overall: 0.019

The filter-to-filter and day-to-day standard deviations (STDEV) are also listed. The negative values are caused by the spectral area being under the baseline.

times lower, indicating consistent absorption of the same filter on different days.

Consistency of particle deposition patterns

RCS quantification by DoF FTIR does not require uniform particle deposition across the filter when the calibration setup mimics the routine sampling configuration, but it requires the deposition pattern to be consistently independent of particle loading (Miller et al. 2013; Chubb and Cauda 2022). Figure 6a shows the Q-values measured from 17 locations on each of the five PVC filters loaded with 84–226 μg RCS. Similar to the results from a 3-piece cassette preceded by a Dorr-Oliver cyclone by Miller et al. (2013), the 3-piece cassette preceded by an aluminum cyclone created an approximate radially symmetric deposition

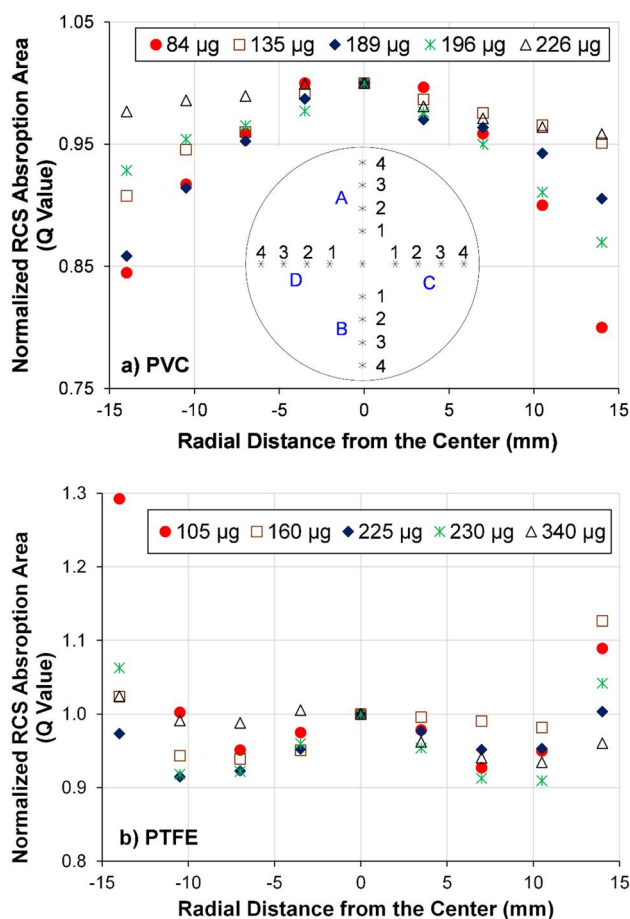


Figure 6. Integrated peak areas of RCS absorption region (Q-value; unitless) at 17 measuring points for (a) five PVC filters and (b) five PTFE filters loaded with different amounts of RCS. The stars inside the circle inset in panel (a) indicate the measurement locations along two perpendicular diameters. The Q-values at positive radial locations were averaged from corresponding A and C locations, while those at negative radial locations were averaged from B and D locations. The plotted Q-values were normalized to those at the center.

pattern. The Q-values were higher at the center and decreased by 5%–20% near the edge. These radial variations are smaller than the 40% drop from the center to 12 mm away from the center of filters reported by Miller et al. (2013), indicating that the particle deposits in this study are more uniform. Although the Q-value radial distribution varies with loading, no consistent loading dependence is observed. The standard deviations of the Q-values at the 17 measurement points were 0.01–0.03, corresponding to an RCS mass of 2.9–8.8 μg , in the same range as the blank filter-to-filter variations.

Similar uniformity measurements were made for five PTFE filters with different RCS loadings (Figure 6b). The Q-value standard deviations across the filter diameter were about 0.05, equivalent to 12 μg RCS. The PTFE filters show a different radial symmetry from PVC filters: the Q-value first slightly decreased from the center but increased again near the edge, probably due to the change of flow pattern near the support ring. Due to the consistent deposition pattern, a single FTIR measurement at the center can provide reasonably accurate RCS concentrations for both PVC and PTFE filters, as demonstrated by high correlations ($R^2 > 0.992$) in Figure 3.

Filtration efficiencies and pressure drops

Figure 7 shows the filtration efficiencies for PVC and PTFE filters. The mean filtration efficiencies are $\geq 98.8\%$ across the measured particle size range. Due to low concentrations of particles $>0.47 \mu\text{m}$ aerodynamic diameter generated by the atomizer, the filtration efficiencies for larger particles were not measured. Even though filters would likely have

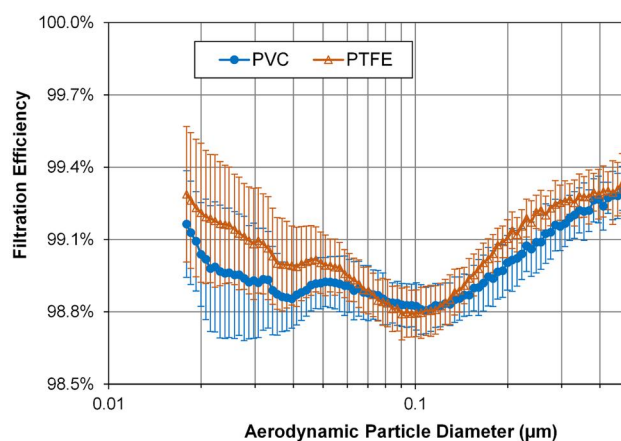


Figure 7. Measured PVC and PTFE filtration efficiencies as a function of particle size. The error bars represent the standard deviation of 9–10 repeated tests for each type of filter.

higher efficiencies for larger particles due to more efficient capture by impaction, gravimetric settling, and interception, future experiments should be conducted to confirm this. Both filters show a most penetrating particle size (MPPS) around $0.1\text{ }\mu\text{m}$ aerodynamic diameter ($0.11\text{ }\mu\text{m}$ for PVC and $0.097\text{ }\mu\text{m}$ for PTFE). These results are similar to those reported by Soo et al. (2016). As most particle masses are present in the size range $>0.3\text{ }\mu\text{m}$ for mining operations (Birch and Noll 2004; Bugarski et al. 2020; Sarver et al. 2021), filtration efficiencies $\geq 98.8\%$ for both filter types are sufficient to collect these particles.

The initial pressure drops for PVC and PTFE filters before particle loading are 0.3 and 0.2 kPa, respectively, lower than the 0.347 and 0.636 kPa reported by Soo et al. (2016). Following the fourth consecutive filtration test after loading with salt particles, the pressure drops increased by 0.05 kPa for both filter types. These pressure drops are much lower than the maximum 7 kPa capacity that the Escort ELF pump can compensate for. As the 37-mm PVC filters have been widely used in mine sampling with the ELF pump without problems regarding excessive pressure drop, the low-pressure drop of the test filters suggests the likelihood of maintaining a stable flow rate for mining sampling over typical work shifts.

Discussion

This study found that the reference spectra variability for blank filters can affect RCS mass quantification. Two approaches can be used for blank correction to reduce bias and uncertainty.

1. Measure the transmittance of the same filter before and after sampling to calculate absorbance using Equation (1). This approach removes the uncertainties caused by filter-to-filter variabilities and takes advantage of the low day-to-day variations. For PVC filters, the LOD and LOQ with this approach are 1.5 and $4.9\text{ }\mu\text{g}/\text{m}^3$, respectively, for most filters, but can be as high as 5.9 and $19.6\text{ }\mu\text{g}/\text{m}^3$, respectively. For PTFE filters, the LOD and LOQ are 1.2 and $4.0\text{ }\mu\text{g}/\text{m}^3$, respectively. This method requires spectra collection with an empty IR chamber in addition to the pre-sample and sample filter measurement (i.e., four spectral measurements). It also requires the pre-sample and sample filter spectra to be measured by the same FTIR instrument, which might be logistically difficult if filters are pre-weighed and packaged by filter suppliers. The absorption by the

filter itself might also change during sampling due to membrane structure changes caused by airflow and/or particle deposition; additional research is needed to evaluate this effect.

2. Use a designated laboratory reference filter of the same type and preferably from the same batch as the sample filter, measure I_{Sample} and $I_{\text{Reference}}$ immediately one after another, and use Equation (2) to calculate absorbance. This method only requires transmittance measurement with the reference and sample filters (i.e., two spectral measurements). However, as shown in Tables 1–3, the blank filter-to-filter variability is approximately one order of magnitude higher than the day-to-day variability, resulting in RCS LODs of 7.4 and $12\text{ }\mu\text{g}/\text{m}^3$ and LOQs of 24.5 and $40\text{ }\mu\text{g}/\text{m}^3$ for 8-hour shift measurement using PVC and PTFE filters, respectively. The PVC LOQ is marginally adequate for the $25\text{ }\mu\text{g}/\text{m}^3$ action level, while the PTFE filter is not suitable to quantify low RCS concentration using DoF FTIR with this blank correction approach. For PVC filters, this variability can be reduced using the filter mass difference between the pre-sample and reference filters and a regression equation similar to those in Figure 5, thereby reducing LOQs. Using a reference filter with a similar mass to the pre-sample filter can also reduce the uncertainties; however, this approach is less practical for a large volume of samples as the pre-sample filter mass will vary from filter to filter. Such corrections are not possible for PTFE filters with a support ring because the blank filter absorption is not correlated with filter mass.

One potential approach to increase the sensitivity and reduce uncertainty is to use filters with a smaller deposit area that will result in higher FTIR signals and lower uncertainties caused by blank subtraction or baseline correction. A novel cyclone by Lee et al. (2017) produced a deposit diameter of 8.8 mm, resulting in the DoF FTIR sensitivity 10 times higher than the Dorr-Oliver cyclone. The Continuous Personal Dust Monitor (CPDM) uses a 13-mm diameter filter, which would increase particle loading per unit area by 8 times as compared to a 37-mm filter. Furthermore, as the FTIR only illuminates a diameter of 6–9 mm of a sample filter (Ashley et al. 2020), a larger fraction of the sample is illuminated for filters with a smaller area, resulting in lower uncertainties caused by variations in the particle deposition pattern. Another approach to increase mass loading is to use higher

flow rates or longer sampling periods if these are allowed by the sampling devices or protocols. Practices to increase particle loading should avoid dust falling off the deposit and excessive pressure drops.

Data presented in this study were obtained from 37-mm SKC GLA-5000 PVC filters and Cytiva PTFE filters from the same batch, and particle collection used a Zefon aluminum cyclone connected with a 3-piece conductive cassette (Figure 1b). Similar characterizations should be performed for other filter media and sampler configurations, and the data could be integrated with the FAST software for wider applications. The reference filters should be selected from the same batch and manufacturer to minimize filter-to-filter variations.

Conclusion

With regulations further lowering RCS limits, rapid and accurate quantifications of RCS are important for timely dust control and exposure mitigation. While the DoF FTIR can provide faster measurements than standard methods, its detection limits need to be evaluated against the lower regulatory limits. This study assessed the impacts of PVC and PTFE filter characteristics on RCS quantification uncertainty.

Both filter types show lower RCS LODs when the pre-sample filter is used as the spectral reference: $5.9 \mu\text{g}/\text{m}^3$ for PVC and $1.2 \mu\text{g}/\text{m}^3$ for PTFE filters. When a designated laboratory blank is used as the reference, the LODs are higher: 7.4 and $12 \mu\text{g}/\text{m}^3$ for PVC and PTFE filters, respectively. For PVC filters, the measured RCS linearly increases by 4.5–5.1 μg for every milligram reference filter mass increase. This relationship can be used to correct the mass differences between the pre-sample (i.e., blank filter before sampling) and reference (i.e., designated laboratory blank) filters thereby reducing LODs. For PTFE filters, the RCS absorption area is not correlated with reference filter mass; therefore, using the pre-sample filter for blank correction is preferred over the designated laboratory reference filter method.

Particle deposition patterns are different on PVC and PTFE filters. However, both show radially symmetric patterns independent of RCS loadings, indicating that reliable RCS quantification can be achieved by measurement at the filter center and a calibration curve derived from a system that mimics routine sampling. Both types of filters show a most penetrating aerodynamic diameter around $0.1 \mu\text{m}$ with filtration efficiencies $\geq 98.8\%$ in the size range of 0.018–

$0.47 \mu\text{m}$ at a flow rate of 2.5 L/min. The pressure drops were within the performance specifications of the ELF pumps. Therefore, both filters are suitable for RCS collection and quantification, however, proper methods are needed to account for the variability of blank absorption among different filters.

Acknowledgments

We want to thank NIOSH researchers Lauren Chubb and Emanuele Cauda for providing additional information about the FAST software and Art Miller for helpful discussions on DoF FTIR analysis.

Disclaimer

The findings and conclusions in this paper are those of the author(s) and do not necessarily represent the official position of the National Institute for Occupational Safety and Health (NIOSH) and the Centers for Disease Control and Prevention (CDC). The mention of any company or product does not constitute endorsement by NIOSH or CDC.

Disclosure statement

No potential conflict of interest was reported by the author(s).

Funding

This study was supported by NIOSH grants 75D30119C0759 and 75D30121C11871.

ORCID

Xiaoliang Wang  <http://orcid.org/0000-0002-2345-7308>

Data availability statement

The data that support the findings of this study are available from the corresponding author upon request.

References

- Abbasi B, Wang XL, Chow JC, Watson JG, Peik B, Nasiri V, Riemenschnitter KB, Elahifard M. 2021. Review of respirable coal mine dust characterization for mass concentration, size distribution and chemical composition. *Minerals*. 11(4):426. doi: [10.3390/min11040426](https://doi.org/10.3390/min11040426).
- ACGIH. 2023. 2023 TLVs and BEIs based on the documentation of the threshold limit values for chemical substances and physical agents and biological exposure indices. Cincinnati (OH): American Conference of Governmental Industrial Hygienists (ACGIH).
- Ashley EL, Cauda E, Chubb LG, Tuchman DP, Rubinstein EN. 2020. Performance comparison of four portable FTIR instruments for direct-on-filter measurement of

- respirable crystalline silica. *Ann Work Expo Health*. 64(5):536–546. doi: [10.1093/annweh/wxaa031](https://doi.org/10.1093/annweh/wxaa031).
- Barnes H, Goh NSL, Leong TL, Hoy R. 2019. Silica-associated lung disease: an old-world exposure in modern industries. *Respirology*. 24(12):1165–1175. doi: [10.1111/resp.13695](https://doi.org/10.1111/resp.13695).
- Bell JL, Mazurek JM. 2020. Trends in pneumoconiosis deaths—United States, 1999–2018. *MMWR Morb Mortal Wkly Rep*. 69(23):693–698.
- Birch ME, Noll JD. 2004. Submicrometer elemental carbon as a selective measure of diesel particulate matter in coal mines. *J Environ Monit*. 6(10):799–806. doi: [10.1039/b407507b](https://doi.org/10.1039/b407507b).
- Blackley DJ, Reynolds LE, Short C, Carson R, Storey E, Halldin CN, Laney AS. 2018. Progressive massive fibrosis in coal miners from 3 clinics in Virginia. *JAMA*. 319(5):500–501.
- Bugarski AD, Hummer JA, Vanderslice S, Shahan MR. 2020. Characterization of aerosols in an underground mine during a longwall move. *Mining Metall Explor*. 37:1065–1078.
- Cauda E, Chubb L, Reed R, Stepp R. 2018. Evaluating the use of a field-based silica monitoring approach with dust from copper mines. *J Occup Environ Hyg*. 15(10):732–742.
- Cauda E, Miller A, Drake P. 2016. Promoting early exposure monitoring for respirable crystalline silica: taking the laboratory to the mine site. *J Occup Environ Hyg*. 13(3):D39–D45.
- Chow JC, Watson JG, Wang X, Abbasi B, Reed WR, Parks D. 2022. Review of filters for air sampling and chemical analysis in mining workplaces. *Minerals*. 12(10):1314. doi: [10.3390/min12101314](https://doi.org/10.3390/min12101314).
- Chubb LG, Cauda EG. 2021. A novel sampling cassette for field-based analysis of respirable crystalline silica. *J Occup Environ Hyg*. 18(3):103–109.
- Chubb LG, Cauda EG. 2022. Direct-on-filter analysis for respirable crystalline silica using a portable FTIR instrument. NIOSH Mining Program Information Circular, IC 9533. Pittsburgh (PA): National Institute for Occupational Safety and Health (NIOSH). <https://www.cdc.gov/niosh/mining/works/cover-sheet2175.html>.
- Cohen RA, Rose CS, Go LHT, Zell-Baran LM, Almberg KS, Sarver EA, Lowers HA, Iwaniuk C, Clingerman SM, Richardson DL, et al. 2022. Pathology and mineralogy demonstrate respirable crystalline silica is a major cause of severe pneumoconiosis in U.S. coal miners. *Ann Am Thorac Soc*. 19(9):1469–1478. doi: [10.1513/AnnalsATS.202109-1064OC](https://doi.org/10.1513/AnnalsATS.202109-1064OC).
- Cytiva. 2024. PTFE membrane disc filters. Marlborough (MA): Cytiva; [accessed 2024 Mar 21]. <https://www.cytivalifesciences.com/en/us/shop/lab-filtration/membranes-discs-sheets-and-reels/ptfe-membranes/ptfe-membrane-disc-filters-p-36483>.
- Farcas D, Lee T, Chisholm WP, Soo J-C, Harper M. 2016. Replacement of filters for respirable quartz measurement in coal mine dust by infrared spectroscopy. *J Occup Environ Hyg*. 13(2):D16–D22.
- Go LHT, Rose CS, Zell-Baran LM, Almberg KS, Iwaniuk C, Clingerman S, Richardson DL, Abraham JL, Cool CD, Franko AD, et al. 2023. Historical shift in pathological type of progressive massive fibrosis among coal miners in the USA. *Occup Environ Med*. 80(8):425–430. doi: [10.1136/oemed-2022-108643](https://doi.org/10.1136/oemed-2022-108643).
- Hart JF, Autenrieth DA, Cauda E, Chubb L, Spear TM, Wock S, Rosenthal S. 2018. A comparison of respirable crystalline silica concentration measurements using a direct-on-filter Fourier transform infrared (FT-IR) transmission method vs. a traditional laboratory X-ray diffraction method. *J Occup Environ Hyg*. 15(10):743–754.
- Hua JT, Rose CS, Redlich CA. 2023. Engineered stone-associated silicosis—a lethal variant of an ancient disease. *JAMA Intern Med*. 183(9):908–910. doi: [10.1001/jamainternmed.2023.3260](https://doi.org/10.1001/jamainternmed.2023.3260).
- Jaenicke R. 1972. The optical particle counter: cross-sensitivity and coincidence. *J Aerosol Sci*. 3(2):95–111.
- Lee T, Lee L, Cauda E, Hummer J, Harper M. 2017. Respirable size-selective sampler for end-of-shift quartz measurement: development and performance. *J Occup Environ Hyg*. 14(5):335–342.
- Lorberau C. 1990. Investigation of the determination of respirable quartz on filter media using Fourier transform infrared spectrophotometry. *Appl Occup Environ Hyg*. 5(6):348–350. doi: [10.1080/1047322X.1990.10389652](https://doi.org/10.1080/1047322X.1990.10389652).
- Miller AL, Drake PL, Murphy NC, Cauda EG, LeBouf RF, Markevicius G. 2013. Deposition uniformity of coal dust on filters and its effect on the accuracy of FTIR analyses for silica. *Aerosol Sci Technol*. 47(7):724–733.
- Miller AL, Drake PL, Murphy NC, Noll JD, Volkwein JC. 2012. Evaluating portable infrared spectrometers for measuring the silica content of coal dust. *J Environ Monit*. 14(1):48–55.
- Miller AL, Murphy NC, Bayman SJ, Briggs ZP, Kilpatrick AD, Quinn CA, Wadas MR, Cauda EG, Griffiths PR. 2015. Evaluation of diffuse reflection infrared spectrometry for end-of-shift measurement of α -quartz in coal dust samples. *J Occup Environ Hyg*. 12(7):421–430.
- Miller AL, Weakley AT, Griffiths PR, Cauda EG, Bayman S. 2017. Direct-on-filter α -quartz estimation in respirable coal mine dust using transmission Fourier transform infrared spectrometry and partial least squares regression. *Appl Spectrosc*. 71(5):1014–1024. doi: [10.1177/0003702816666288](https://doi.org/10.1177/0003702816666288).
- MSHA. 2008. Infrared determination of quartz in respirable coal mine dust—method No. MSHA P7. Pittsburgh (PA): Mine Safety Health Administration, Department of Labor. <https://arlweb.msha.gov/TECHSUPP/pshtcweb/MSHA%20P7.pdf>.
- MSHA. 2024. Lowering miners' exposure to respirable crystalline silica and improving respiratory protection. Federal Register 89 (76): Mine Safety and Health Administration (MSHA). 89 (76). <https://www.govinfo.gov/content/pkg/FR-2024-04-18/pdf/2024-06920.pdf>.
- Nascimento P, Taylor SJ, Arnott WP, Kocsis KC, Wang XL, Firouzkouhi H. 2022. Development of a real-time respirable coal dust and silica dust monitoring instrument based on photoacoustic spectroscopy. *Mining Metall Explor*. 39:2237–2245.
- NIOSH. 2003. Quartz in coal mine dust, by IR (redemption)—NIOSH Method 7603. NIOSH Manual of Analytical Methods (NMAM), Fourth Edition. Washington (DC): The National Institute for Occupational Safety and Health (NIOSH). <https://www.cdc.gov/niosh/docs/2003-154/pdfs/7603.pdf>.

- OSHA. 2016. Occupational exposure to respirable crystalline silica. Federal Register 81 (58): Occupational Safety and Health Administration (OSHA). <https://www.govinfo.gov/content/pkg/FR-2016-03-25/pdf/2016-04800.pdf>.
- Pampena JD, Cauda EG, Chubb LG, Meadows JJ. 2020. Use of the field-based silica monitoring technique in a coal mine: a case study. *Mining Metall Explor.* 37(2):717–726.
- Sarver E, Keleş Ç, Afrouz SG. 2021. Particle size and mineralogy distributions in respirable dust samples from 25 US underground coal mines. *Int J Coal Geol.* 247:103851.
- SKC. 2024. GLA 5000 PVC membrane filters. Eighty Four (PA): SKC Inc; [accessed 2024 Mar 21]. <https://www.skccinc.com/categories/gla-5000-pvc-membrane-filters>.
- Soo J-C, Monaghan K, Lee T, Kashon M, Harper M. 2016. Air sampling filtration media: collection efficiency for respirable size-selective sampling. *Aerosol Sci Technol.* 50(1):76–87.
- Stacey P, Kauffer E, Moulut J-C, Dion C, Beuparlant M, Fernandez P, Key-Schwartz R, Friede B, Wake D. 2009. An international comparison of the crystallinity of calibration materials for the analysis of respirable α -quartz using x-ray diffraction and a comparison with results from the infrared kbr disc method. *Ann Occup Hyg.* 53(6):639–649.
- Stach R, Barone T, Cauda E, Krebs P, Pejčić B, Daboss S, Mizaikoff B. 2020. Direct infrared spectroscopy for the size-independent identification and quantification of respirable particles relative mass in mine dusts. *Anal Bioanal Chem.* 412(14):3499–3508.
- U.S. EPA. 2016. Technical assistance document for the National Air Toxics Trends Stations Program—revision 3. Research Triangle Park (NC): Office of Air Quality Planning and Standards, U.S. Environmental Protection Agency; [accessed 2020 May 20]. https://www3.epa.gov/ttnamti1/files/ambient/airtox/NATTS%20TAD%20Revision%203_FINAL%20October%202016.pdf.
- Vanka KS, Shukla S, Gomez HM, James C, Palanisami T, Williams K, Chambers DC, Britton WJ, Ilic D, Hansbro PM, et al. 2022. Understanding the pathogenesis of occupational coal and silica dust-associated lung disease. *Eur Respir Rev.* 31(165):210250. doi: 10.1183/16000617.0250-2021.
- Wang SC, Flagan RC. 1990. Scanning electrical mobility spectrometer. *Aerosol Sci Technol.* 13:230–240.
- Wang XL, Chancellor G, Evenstad J, Farnsworth JE, Hase A, Olson GM, Sreenath A, Agarwal JK. 2009. A novel optical instrument for estimating size segregated aerosol mass concentration in real time. *Aerosol Sci Technol.* 43(9):939–950.
- Wang XL, Zhou H, Arnott WP, Meyer ME, Taylor S, Firouzkouhi H, Moosmüller H, Chow JC, Watson JG. 2020. Evaluation of gas and particle sensors for detecting spacecraft-relevant. *Fire Emissions Fire Saf J.* 113(102977):1–12.
- Watson JG, Tropp RJ, Kohl SD, Wang XL, Chow JC. 2017. Filter processing and gravimetric analysis for suspended particulate matter samples. *Aerosol Sci Eng.* 1(2):93–105. doi: 10.1007/s41810-017-0010-4.
- Wolfe C, Chubb L, Walker R, Yekich M, Cauda E. 2022. Monitoring worker exposure to respirable crystalline silica: application for data-driven predictive modeling for end-of-shift exposure Assessment. *Ann Work Expo Health.* 66(8):1010–1021. doi: 10.1093/annweh/wxac040.